Modeling and Predicting Climate Parameters in Guinea using Simple Perceptrons: A Study on Temperature and Precipitation

Katakpe Kossi Kuma
UL, Université de Labé, Guinée

Camara Moustapha N'gonet
UL, Université de Labé, Guinée.
UGANC, Université Gamal Abdel Nasser de Conakry, Guinée

Sow Abdoulaye
UL, Université de Labé, Guinée

Kpoghomou Pépé
UL, Université de Labé, Guinée

Makanera Mohamed
UL, Université de Labé, Guinée

ABSTRACT
The climate in Guinea, like many regions around the world, is undergoing significant changes, impacting ecosystems, human societies, and local economies. Accurate forecasting of climate parameters, such as temperature and precipitation, is essential for managing climate-related risks and informing environmental and agricultural policies. This study explores the use of simple perceptrons, a type of artificial neural network, to model and predict temperature and precipitation patterns in Guinea. The data used for training and testing the model comes from historical climate records collected from various meteorological stations across the country over several years.

The methodology is based on the classic architecture of simple perceptrons, with a gradient descent learning algorithm and an adapted error function. The results indicate that the model is capable of predicting temperature fluctuations and precipitation levels with satisfactory accuracy, though improvements are needed for better performance, particularly for long-term predictions. When compared to traditional climate modeling methods, the simple perceptron approach shows promising results, while also revealing limitations due to the complexity of the region's climatic phenomena.

These findings open the door for future research to explore more advanced neural network structures, such as multilayer networks, and to incorporate additional variables to enhance predictions on a larger scale and for longer time horizons. This study contributes to the growing body of knowledge on applying artificial intelligence techniques to climate forecasting, with a particular focus on the specific climatic conditions of Guinea.

Keywords
Climate Prediction, Simple Perceptrons, Temperature Forecasting, Precipitation Modeling, Guinea Climate

1. INTRODUCTION
Climate change is one of the greatest threats facing the world today, as it induces variations in temperature and precipitation that affect ecosystems, biodiversity, and food security, particularly in vulnerable regions such as Africa. In Guinea, as in many other tropical areas, these climatic phenomena have significant impacts on agriculture, water resources, health, and infrastructure. To better understand and anticipate these impacts, climate parameter modeling has become essential, as it allows for the prediction of future climate changes and facilitates the adaptation of resource management strategies and risk prevention measures.

At the core of climate modeling are mathematical and computational models, which simulate climate variations across different temporal and spatial scales. For instance, Schmidt (2006) emphasizes that climate models integrate numerous physical interactions and are used to simulate climate variability within the ocean-atmosphere system; these models rely on numerical representations of the climate system [1]. Similarly, the Intergovernmental Panel on Climate Change (IPCC) notes that climate models are implemented as computer codes running on powerful computers, capable of reproducing observed aspects of climate across seasonal to decadal temporal scales and across diverse spatial scales (IPCC, 2007) [2].

Despite these advances, accelerated progress in climate modeling remains necessary to support effective climate change adaptation. Key small-scale processes, such as turbulence and cloud formation, cannot yet be explicitly resolved and therefore require parameterizations. In this context, a combined approach that leverages traditional process-based parameterizations alongside artificial intelligence (AI)-based methods has been proposed to improve the accuracy, interpretability, and reliability of climate predictions [3].

Building on these modeling advances, recent studies have investigated the impacts of climate change and sea level rise on coastal aquifers, employing integrated modeling systems to simulate groundwater and seawater intrusion under different climate scenarios (RCP4.5 and RCP8.5). The results indicate that seawater intrusion is projected to increase in the future, with varying patterns in groundwater recharge and sensitivity to changes in the components of the water cycle [4]. Such findings highlight the importance of sophisticated modeling approaches to understand regional climate impacts and to design effective adaptation strategies.

Recent advances in AI, particularly in neural networks and machine learning, have transformed multiple fields, including climate forecasting. AI enables the processing of large and complex climate datasets, allowing for the extraction of meaningful patterns and the generation of accurate short- and long-term predictions. Neural networks, such as perceptrons, are capable of learning complex relationships between climatic

variables, which can result in faster and more accurate predictions compared to traditional statistical or physical methods, Hewitson et al. [5]. Moreover, in 2018, Rasp et al.'s studies have demonstrated that deep neural networks trained on outputs from climate models can outperform persistence forecasts and enhance prediction accuracy over extended periods, highlighting their ability to capture intricate climate interactions [6]. These networks, particularly in deep learning architectures, can represent nonlinear subgrid processes and improve forecast reliability relative to conventional parameterizations [7], Weber et al., 2020. Such approaches are especially valuable in regions like Guinea, where climate data is often sparse or fragmented, and traditional models face challenges in accurately capturing local climate dynamics.

For this study, simple perceptrons, a basic type of artificial neural network, were chosen due to their simplicity and efficiency in classification and regression tasks. As noted by Haykin et al. [8], although perceptrons are less complex than multilayer networks, they can produce satisfactory results for prediction problems where the relationships between input and output variables are relatively linear. In climatology, where many parameters are interconnected in complex but often linear ways, Haykin highlights that simple perceptrons provide a pragmatic and effective approach for modeling short-term variations in temperature and precipitation.

Solomatine et al. [9], observed that, traditionally, physically based models relying on mathematical descriptions of water movement have been widely used in river basin management. They note that, in the past decade, data-driven models based on computational intelligence and machine learning have become increasingly common. These models require substantial datasets representing the system's physics and have shown promising applications, though they also present challenges and pitfalls that are still being addressed in ongoing research.

In addition, Hsu et al. [10], demonstrated that artificial neural networks (ANNs) are flexible mathematical structures capable of capturing complex nonlinear relationships between inputs and outputs, particularly when physical equations are insufficient to fully describe the system. They showed that three-layer feedforward ANN models, identified using a linear least squares simplex (LLSSIM) procedure, can effectively simulate rainfall-runoff dynamics in watersheds and outperform linear time series or conceptual models for input-output forecasting. However, these authors emphasize that ANNs do not replace physically based watershed models but offer a viable, computationally efficient, and interpretable alternative.

Taken together, these studies indicate that the use of simple perceptrons and ANNs not only reduces computational overhead compared to more complex neural networks but also maintains interpretability, which is particularly advantageous for applied climatology and hydrology in regions with limited or fragmented data.

The primary objective of this study is to develop and assess a climate forecasting model based on simple perceptrons, with a focus on predicting temperature and precipitation in Guinea. Specifically, the research seeks to evaluate the capability of simple perceptrons to accurately forecast short-term climate variations within a local context, compare their performance with that of traditional climate forecasting methods, and offer recommendations for enhancing the accuracy of climate predictions through artificial intelligence. The findings from this study are expected to support the implementation of more effective resource management strategies in Guinea, particularly in sectors such as agriculture, water management, and climate risk mitigation.

2. LITERATURE REVIEW

2.1 Classical Climate Modeling Methods

Classical climate modeling methods include statistical models, dynamic models, and empirical approaches. Statistical models are based on established relationships between historical climate variables to predict future conditions. For example, Ghil et al. [11] showed that statistical models can provide short-term climate forecasts, but with limited accuracy when climate variability is high. On the other hand, dynamic models rely on equations of fluid dynamics and thermodynamics to simulate large-scale climate processes. Bretherton et al. [12], emphasized the importance of these models in understanding global phenomena like El Niño and ocean-atmosphere interactions. However, these models are often complex and require large amounts of data for calibration.

Empirical climate models rely on direct observations and statistical relationships between variables such as temperature and precipitation. While these models are relatively simple, they have demonstrated limitations in predicting extreme events and long-term climate trends [13]. Parker further emphasizes that climate model predictions are inherently uncertain and difficult to justify for certain aspects particularly extremes and long-term projections due to intrinsic model imperfections and the complexity of the climate system [14].

Current climate models (GCMs/ESMs) face additional limitations, notably coarse spatial resolution, which hinders the explicit representation of key processes, including extreme events, and contributes to uncertainties in long-term forecasts and climate change projections [13] . In response, scientists have proposed significant reforms to climate modeling, focusing on three complementary approaches: the unified approach (accelerated development of high-resolution models), the hierarchy approach (systematic study of related model hierarchies), and the pluralist approach (increasing diversity in modeling, including empirical methods). While these approaches offer valuable synergies, resource constraints make it unlikely that all will be fully implemented, highlighting the need for more modest, achievable improvements that can still yield substantial benefits.

Weather and climate extremes are a central focus of the World Climate Research Programme (WCRP) Grand Challenge, emphasizing the necessity for improved understanding, modeling, and prediction of extreme events. Advances depend on analyzing large-scale drivers, local-to-regional feedback processes, and stochastic dynamics, with specific strategies for short- and long-duration extremes to enhance predictive skill and model evaluation [15]. Literature reviews indicate that extreme events remain difficult to predict accurately due to model resolution limits, unresolved local feedbacks, and inadequately represented physical processes.

With the growing complexity of the climate system and the increasing availability of observational data, classical modeling methods often struggle to capture nonlinear relationships, motivating the development of new approaches based on artificial intelligence to improve prediction of extreme events and climate variability.

2.2 Introduction to Artificial Neural Networks

Artificial Neural Networks (ANNs), a core branch of artificial intelligence, have increasingly attracted attention in scientific

and engineering disciplines due to their remarkable ability to model complex and nonlinear relationships between input and output variables [16], [17]. Fundamentally, as highlighted by Rumelhart, Hinton, and Williams, an artificial neural network consists of multiple layers of interconnected processing units, or neurons, which communicate via weighted connections and transform input data using nonlinear activation functions. Typically, these networks are trained through supervised learning algorithms that iteratively adjust the connection weights to minimize the discrepancy between predicted and observed outputs.

Among these learning procedures, back-propagation plays a pivotal role by iteratively adjusting weights to reduce output errors. This enables hidden units to capture critical features of the task domain and encode underlying regularities, setting back-propagation apart from earlier methods such as the perceptron-convergence procedure [18]. The perceptron theory, introduced by Rosenblatt et al. [19], provides a conceptual model of a hypothetical nervous system, linking biophysics and psychology to quantitatively predict learning and memory processes, and illustrating how stored information influences recognition and behavior.

Advancements in network architectures further demonstrate the expressive power of ANNs. Standard multilayer feedforward networks with at least one hidden layer are capable of approximating any Borel measurable function to arbitrary accuracy, effectively functioning as universal approximators [20]. Moreover, continuous feedforward networks with a single hidden layer and a continuous sigmoidal activation can uniformly approximate any continuous function and represent arbitrary decision regions, addressing fundamental questions of representability in single-layer networks [21],[22].

Building on these theoretical foundations, modern resources provide comprehensive introductions to deep learning for both beginners and practitioners. For instance, Goodfellow et al. [17], present a structured overview of fundamental mathematical tools, well-established algorithms, and emerging research directions, illustrating the wide applicability of deep learning across domains such as computer vision, natural language processing, robotics, bioinformatics, and beyond.

The perceptron, pioneered by Rosenblatt since 1958 [23], stands as one of the earliest formalized neural network models, designed to perform binary linear classification through a single layer of artificial neurons. Despite its architectural simplicity and its inherent limitation to linearly separable problems, the perceptron laid a critical theoretical and computational groundwork upon which subsequent, more expressive architectures were built [24], [25]. Building upon this foundation, multilayer perceptrons (MLPs) were developed by incorporating one or more hidden layers between the input and output, endowing the network with the capacity to model highly nonlinear and complex functional mappings Hornik et al. [20]. This representational power is rigorously formalized by the universal approximation theorem, which establishes that a sufficiently large MLP can approximate any continuous function to an arbitrary degree of accuracy [21], [26], thereby positioning ANNs as a general-purpose approximation framework.

The application of ANNs to climate science has garnered considerable attention over the past three decades. Haykin et al. [8] noted that neural networks are particularly well-suited for extracting latent patterns from high-dimensional climate and meteorological datasets, without requiring explicit formulation of the underlying physical laws governing the system. This data-driven flexibility is especially valuable in atmospheric and oceanic modeling, where complex nonlinear dynamics and feedback mechanisms render traditional parametric approaches insufficient Hsieh et al. [27] . Empirical studies have confirmed the efficacy of ANNs across a range of climate-related prediction tasks, including rainfall estimation [28], surface temperature forecasting [29] , and the modeling of large-scale climate indices Gardener et al., [30]. Their inherent adaptability to non-stationary and heterogeneous input data further reinforces their suitability for both short-term meteorological forecasting and long-term climate projection Maier et al. [31].

More recent investigations have considerably broadened the scope of ANN applications in climate research. Maqsood et al. [32] demonstrated that multilayer perceptrons (MLPs), alongside other machine learning algorithms such as support vector regression and random forest, can effectively perform statistical downscaling of global climate model outputs for both temperature and precipitation, outperforming conventional statistical downscaling models across multiple climate scenarios (RCP 2.6, RCP 4.5, and RCP 8.5). Building on this, Balmaceda-Huarte et al. [33] showed that convolutional neural networks applied to downscaling daily temperatures over South America successfully captured regional climatic variability under future climate change scenarios, resolving local features that coarser numerical models typically fail to represent. Hsu et al. [34] further demonstrated that neural networks outperform conventional regression techniques in modeling nonlinear interdependencies among climatic variables. Collectively, these contributions underscore the substantial potential of ANNs as robust, scalable tools for enhancing the accuracy and interpretability of climate predictions, particularly as the complexity and volume of environmental observational data continue to grow Abiodun et al. [35].

2.3 Existing Work on Climate Prediction with Neural Networks

Numerous studies have demonstrated the effectiveness of neural networks in improving climate forecasting across diverse geographic and climatic contexts. Citakoglu et al. [36], employed feedforward and Elman neural network models to predict long-term monthly minimum, maximum, and mean air temperatures across 81 meteorological stations in Türkiye, using a dataset spanning nearly a century (1927-2021). Their study confirmed that ANN-based architectures consistently outperform conventional statistical approaches for short- and long-term temperature estimation, particularly in capturing nonlinear relationships that classical parametric models fail to resolve. In sub-Saharan Africa, neural networks have demonstrated considerable promise for seasonal precipitation forecasting. Appiah-Badu et al. [37], investigated the suitability of Long Short-Term Memory (LSTM) recurrent neural networks for monthly rainfall forecasting across multiple ecological zones of Ghana, West Africa. Their results showed that both univariate and multivariate LSTM models performed well in capturing seasonal precipitation patterns, significantly outperforming classical statistical approaches in terms of correlation coefficient (R), Nash-Sutcliffe efficiency, RMSE, and MAE confirming the superiority of deep learning architectures over traditional regression methods for rainfall prediction in data-scarce West African environments. Similarly, Shiri et al. [38] utilized simple perceptrons to forecast precipitation in Southeast Asia, achieving results comparable to classical methods while significantly reducing computational overhead.

More recent investigations have further confirmed and

extended these findings. Ogunrinde et al. [39] applied ANN models to forecast the Standardized Precipitation and Evapotranspiration Index across multiple agroecological zones in Nigeria, demonstrating that ANNs can effectively model drought-related climate indices in data-sparse West African environments. Building on this, Aïzansi et al. [40] conducted a comparative study of multilayer perceptron (MLP) and Long Short-Term Memory (LSTM) networks for monthly rainfall prediction in Benin, West Africa, revealing that both architectures achieved strong predictive accuracy across stations with varying climate regimes, with LSTM models proving particularly suited to capturing temporal dependencies in rainfall sequences. At a broader scale, Guo et al. [41] proposed a hybrid CNN-LSTM model for monthly prediction of six simultaneous climatic variables including temperature, precipitation, and relative humidity over a 72-year dataset in China, demonstrating that deep learning architectures substantially outperform standalone ANN, RNN, and CNN models in terms of RMSE, MAE, and correlation coefficient. In a complementary study, Fan et al. [42] applied neural network post-processing techniques to improve week-3–4 precipitation and 2-meter temperature forecasts from the NOAA/NCEP Climate Forecast System, showing that nonlinear ANN-based methods outperform conventional linear bias-correction approaches, particularly for extended-range forecasts where linear assumptions break down.

Taken together, these studies spanning West Africa, Asia, and global climate systems confirm the growing relevance of neural network approaches for climate prediction, and underscore the particular value of such methods in regions with limited data infrastructure, such as Guinea, where flexible, data-driven architectures offer a pragmatic path toward reliable short- and medium-term climate forecasting.

2.4 Identified Limitations and Positioning of Our Approach

Despite the demonstrated effectiveness of neural networks in climate forecasting, several important limitations have been identified in the literature that must be carefully considered when designing and applying such models. A first well-documented challenge concerns overfitting, particularly in low-data regimes. Lim et al. [43] emphasized that the flexibility of machine learning methods can be a double-edged sword, making them prone to overfitting, and that simpler models may perform better when only a small number of historical observations is available a situation that is especially common in climate forecasting contexts. This observation is particularly relevant for simple neural architectures such as perceptrons, which, while computationally efficient, may struggle to generalize when trained on limited or noisy datasets.

A second limitation concerns the inherent difficulty of modeling nonlinear and long-range climatic dependencies. Shen et al. [44] highlighted that major challenges in applying machine learning to climate prediction include the scarcity of datasets, physical inconsistency, and a lack of model transparency and interpretability limitations that are especially pronounced when predicting sub-seasonal to decadal climate variability. Furthermore, Materia et al. [45], noted that neural networks used for climate extreme prediction face significant constraints due to data scarcity, particularly because the limited occurrence of extreme events in historical records reduces the volume of labeled training samples available for model learning.

A third and perhaps most critical limitation for the present study relates to the availability and quality of climate data in African contexts. Kaspar et al. [46], documented that long time series of weather observations remain sparse across many sub-Saharan African countries, with persistent gaps in observing networks, outdated or non-functional meteorological stations, and insufficient institutional capacity for climate data management all of which directly affect the reliability of data-driven prediction models. These structural challenges are further compounded by the scarcity of high-quality, localized climate data across the continent, limited access to digital infrastructure, and gaps in technical expertise, which together constitute major barriers to the effective deployment of AI-based climate models in Africa.

In this study, the authors aim to address these limitations by applying simple perceptron specifically calibrated to the available climate data in Guinea. The proposed approach adopts a pragmatic strategy that balances model simplicity with rigorous data preprocessing, including imputation of missing values, normalization, and careful train-test splitting. By deliberately choosing a lightweight architecture, the model reduces the risk of overfitting while maintaining interpretability a critical requirement in applied climatology for data-scarce environments. The present work also serves as a baseline study, laying the groundwork for future investigations using more complex architectures, such as multilayer perceptron or LSTM networks, to further improve long-term forecast accuracy in the region.

3. DATA AND PREPROCESSING

3.1 Description of the Data

The data used in this study comes from several meteorological stations located across Guinea. This data covers a period of 10 years, from 2015 to 2024, and includes monthly recordings of temperature (average monthly maximum and minimum temperatures) and precipitation (monthly total precipitation). The data is sourced from the National Directorate of Meteorology of Guinea, which collects these records through a network of meteorological stations distributed throughout the country. Temperatures are expressed in Celsius (°C), while precipitation is measured in millimeters (mm). These two climate parameters are crucial for analyzing short and medium-term climate trends, especially in agricultural regions where these factors directly influence crop production and water resources.

3.2 Data Cleaning and Normalization

Before being incorporated into the forecasting models, the raw climate data collected from the meteorological stations of Guinea underwent a rigorous multi-step preprocessing procedure designed to ensure its quality, completeness, and internal consistency. First, a systematic identification and treatment of missing values was performed, as certain observation periods exhibited data gaps attributable to equipment malfunctions at meteorological stations or errors in the data collection process. Depending on the temporal proximity of available surrounding observations, missing values were addressed either through monthly average imputation, where a gap was isolated and non-systematic, or through linear interpolation, where consecutive missing values could be reliably estimated from adjacent time steps. Second, a correction of anomalous records was carried out by comparing each observed temperature and precipitation value against established historical climate thresholds specific to each station, thereby detecting and rectifying extreme outliers that could distort model training and degrade predictive performance. Third, a cross-station consistency check was conducted, in which temperature and precipitation records from

different meteorological stations were systematically compared to verify their geographical and temporal coherence, ensuring that spatial gradients in the data accurately reflected the known climatic variability across Guinea's diverse topographic and ecological zones. Together, these preprocessing steps constituted an essential foundation for the reliability and robustness of the subsequent modeling and forecasting analyses.

Once the data was cleaned, it was normalized to ensure comparability between the temperature and precipitation variables. Normalization was done using the min-max normalization formula, which scales each variable to a range of $[0, 1]$, which is crucial for neural network models:

$$X_{\text{norm}} = \frac{X - X_{\text{min}}}{X_{\text{max}} - X_{\text{min}}} \quad (1)$$

Where:

- ✓ X_{norm} is the normalized value of the variable,
- ✓ X is the original value of the variable,
- ✓ X_{min} is the minimum value of the variable,
- ✓ X_{max} is the maximum value of the variable.

This normalization ensures that both temperature and precipitation variables are treated equivalently, without one dominating the other due to their respective scales.

3.3 Data Split (Training, Testing, Validation)

To evaluate the model's performance, the data was divided into three distinct subsets: a training set, a testing set, and a validation set.

Training Set: 70% of the data was used to train the perceptron model. This subset allowed the model to learn the relationships between the input variables (temperature and precipitation) and the output (predictions of future temperatures and precipitation). The size of the training set was calculated using the following formula:

$$N_{\text{train}} = 0.7 \times N_{\text{total}} \quad (2)$$

Where N_{train} is the number of data points in the training set, and N_{total} is the total number of available data points.

- ✓ Testing Set: 20% of the data was reserved for testing the model's performance after training. This subset was used to assess how well the model generalizes its predictions on data it has never seen before. The size of the testing set is given by :

$$N_{\text{test}} = 0.2 \times N_{\text{total}} \quad (3)$$

- ✓ Validation Set: 10% of the data was used for validation to fine-tune the model's parameters and avoid overfitting. The size of this set is given by:

$$N_{\text{val}} = 0.1 \times N_{\text{total}} \quad (4)$$

The data splitting was done randomly while maintaining the temporal order of the data to avoid any information leakage between the training and testing sets, which is crucial for time-series forecasting. The data preprocessing steps, including cleaning, normalization, and splitting, are essential to ensure the quality of the model's results. By applying mathematical formulas for normalization and a systematic approach to data splitting, splitting, these steps ensure that the variables are properly prepared, allowing the model to reliably predict climate parameters for Guinea. These steps also enable robust performance validation for the model.

4. METHODOLOGY

4.1 Theory of Simple Perceptrons

A simple perceptron is a type of artificial neural network composed of a single layer of neurons. This model is primarily used for binary classification tasks and linear regression. The perceptron works by taking a linear combination of the inputs and then applying an activation function to produce the output. The general formula for a simple perceptron is:

$$y = f(\sum_{i=1}^{n} w_i x_i + b) \quad (5)$$

Where:

- ✓ y is the perceptron output,
- ✓ f is the activation function (commonly a threshold or sigmoid function),
- ✓ x_i are the inputs (here, climatic parameters like temperature and precipitation),
- ✓ w_i are the weights associated with the inputs,
- ✓ b is the bias, and
- ✓ n is the number of inputs.

This structure allows the perceptron to model simple linear relationships. However, for more complex nonlinear relationships, multilayer networks are needed. The perceptron is used here in the context of regression to predict continuous values for temperature and precipitation.

4.2 Model Architecture Used

In this study, a simple perceptron with a single layer and a single output unit was used to predict climate parameters. The model consists of two main layers: an input layer, which takes the climatic variables such as temperature and precipitation from past periods, and an output layer, which generates the prediction for future temperature or precipitation.

The architecture of the simple perceptron used in this study can be represented as follows:

$$\mathbf{y} = f(\mathbf{W} \cdot \mathbf{X} + \mathbf{b}) \quad (6)$$

Where:

- ✓ $\mathbf{X}$ is the input vector (temperature and precipitation),
- ✓ $\mathbf{W}$ is the weight matrix,
- ✓ $\mathbf{b}$ is the bias,
- ✓ $\mathbf{y}$ is the predicted output (future temperature or precipitation),
- ✓ f is the activation function applied to the outputs.

The most commonly used activation function in this case is the linear function for regression, but other functions may be used depending on the nature of the data.

4.3 Learning Algorithm (Gradient Descent, Error Function, etc.)

Learning in a simple perceptron is achieved using the gradient descent method. The goal is to minimize the error between the values predicted by the model and the actual observed values by adjusting the weights $\mathbf{W}$ and the bias $\mathbf{b}$. The most commonly used error function is the Mean Squared Error (MSE), which is defined by the following formula:

$$\text{MSE} = \frac{1}{N}\sum_{i=1}^{N}(y_i - \hat{y}_i)^2 \quad (7)$$

Where:

- ✓ y_i is the true value,
- ✓ $\hat{y}_i$ is the predicted value by the model,
- ✓ N is the number of samples in the dataset.

Gradient descent is used to minimize this error function by updating the perceptron weights based on the gradient of the error with respect to the weights, using the following update

rule:

$$w_i = w_i - \eta \frac{\partial \text{MSE}}{\partial w_i} \quad (8)$$

Where:

- ✓ η is the learning rate, which determines the step size of each update,
- ✓ $\frac{\partial \text{MSE}}{\partial w_i}$ is the gradient of the error with respect to the weight w_i.

The weights are iteratively adjusted during training until the error is minimized.

4.4 Experimental Scenarios

To evaluate the performance of the simple perceptron in predicting climate parameters, three experimental scenarios were designed. In the first scenario (univariate prediction), the model used only past values of a single variable (temperature or precipitation) to forecast its future, assessing its ability to capture simple temporal dependencies. The second scenario (multivariate prediction) combined temperature and precipitation as inputs, examining the effect of cross-variable interactions on prediction accuracy. The third scenario compared short-term (monthly) and long-term (annual) forecasts to evaluate the model's temporal stability.

This methodology, combining the perceptron, gradient descent optimization, and progressively structured experiments, provides a comprehensive assessment of the model's strengths and limitations for climate prediction in Guinea.

5. RESULTS AND DISCUSSION

5.1 Model Performance

The performance of the Simple Perceptron (SGD) model was evaluated across all 34 prefectures of Guinea using three complementary metrics: the Root Mean Square Error (RMSE), the Mean Absolute Error (MAE), and the coefficient of determination (R^2). These metrics were computed on denormalized (original-scale) values for three experimental scenarios: (1) univariate temperature prediction, (2) univariate precipitation prediction, and (3) multivariate prediction combining both variables, each evaluated on the chronological test set corresponding to the final 20% of the historical data (2015–2024). Complete prefecture-level results are provided in Appendix A (Tables A1 and A2).

Table 1. Summary performance statistics of the Simple Perceptron (SGD) across all 34 prefectures of Guinea: Univariate and Multivariate scenarios, chronological test set

Scenario & Variable	Metric	Mean	SD	Min	Max
Univariate Temperature (°C)	RMSE	1.441	0.350	**0.803**	**1.935**
	MAE	1.195	0.296	**0.667**	**1.592**
	R^2	0.548	0.202	**0.028**	**0.715**
Univariate Precipitation (Mm)	RMSE	108.64	17.22	**78.38**	**153.17**
	MAE	85.28	13.06	**61.93**	**116.08**
	R^2	0.669	0.050	**0.572**	**0.756**
Multivariate Temperature (°C)	RMSE	1.544	0.482	**0.642**	**2.143**
	MAE	1.335	0.370	**0.504**	**1.836**
	R^2	0.535	0.100	**0.404**	**0.690**
Multivariate Precipitation (Mm)	RMSE	93.06	16.49	**61.77**	**120.35**
	MAE	72.83	12.36	**50.00**	**90.60**
	R^2	0.753	0.058	**0.619**	**0.832**

Table 1 presents the complete summary statistics of model performance across all 34 prefectures for the four prediction scenarios. Several key observations emerge from this dataset. The standard deviation of R^2 across prefectures is notably higher for temperature (SD = 0.202) than for precipitation (SD = 0.050), indicating that temperature predictability is far more spatially heterogeneous across Guinea's territory. This contrast reflects the diversity of local thermal regimes, ranging from the stable maritime climate of the Atlantic coast to the highly variable continental climate of Upper Guinea. For precipitation, the lower inter-prefecture dispersion (SD = 0.050) confirms that the dominant monsoon signal imposes a more uniform seasonal structure across the country, making precipitation prediction more consistently achievable regardless of geographic location.

In the univariate temperature prediction scenario, the model achieves a national mean RMSE of 1.441°C (SD = 0.350), a mean MAE of 1.195°C, and a mean R^2 of 0.548. The best-performing prefecture is Lelouma (Futa Jallon region, R^2 = 0.715, RMSE = 1.255°C), while the worst-performing prefectures are the coastal cluster of Boffa, Conakry, Fria, and Dubreka (Maritime Guinea, R^2 = 0.028), reflecting the dominant influence of Gulf of Guinea sea-surface temperature variability that the autoregressive lag features cannot capture. Full prefecture-level details are provided in Table A1 (Appendix A).

In the univariate precipitation prediction scenario, the model yields a national mean RMSE of 108.64 mm (SD = 17.22), a mean MAE of 85.28 mm, and a mean R^2 of 0.669. Despite

substantially higher absolute errors compared to temperature, the R^2 values are markedly higher (0.669 vs. 0.548), indicating that the model captures a greater proportion of the seasonal precipitation variance. This reflects the dominant amplitude of the annual monsoon cycle relative to inter-annual variability. This result may appear counter-intuitive, as precipitation is generally considered a more irregular and harder-to-predict variable than temperature. However, this apparent paradox is explained by the nature of the variance being modeled: in Guinea, monthly precipitation is dominated by a strong and highly regular unimodal monsoon cycle, with near-zero values during the dry season (November-April) and a pronounced peak during the rainy season (June-September). This large-amplitude seasonal signal is readily captured by autoregressive lag features, yielding high R^2 values despite large absolute errors in millimeters. In contrast, monthly temperature varies within a narrower absolute range (approximately 4-6°C between seasons depending on the region), and its inter-monthly variability contains a higher proportion of irregular, non-seasonal fluctuations that the linear perceptron cannot resolve, resulting in a lower R^2 despite smaller absolute errors. The best precipitation predictability is recorded in Kerouane and Beyla (Forest Guinea, $R^2 = 0.756$), while the lowest is in Siguiri and Mandiana (Upper Guinea, $R^2 = 0.572$). Complete prefecture-level results are provided in Table A2 (Appendix A).

Under the multivariate scenario, incorporating cross-variable lag features produces asymmetric effects. For temperature, the multivariate approach yields a slight degradation (mean R^2 from 0.548 to 0.535, -2.4%; RMSE from 1.441°C to 1.544°C, +7.1%), suggesting that precipitation lags introduce feature noise for the linear temperature model. For precipitation, the multivariate scenario produces a substantial improvement (mean R^2 from 0.669 to 0.753, +12.6%; RMSE from 108.64 mm to 93.06 mm, -14.3%), confirming that temperature lags carry significant cross-variable predictive information for precipitation, consistent with the coupling between moisture convergence and near-surface temperature in the West African Monsoon system.

Table 2. Short-term and Long-term temperature prediction: SGD National summary statistics.

Horizon	Mean RMSE (°C)	Mean MAE (°C)	Mean R^2	Best Prefecture (R^2)
Short-Term (h = 1 month)	1.441	1.195	0.548	Lelouma (0.715)
Long-Term (h = 12 months)	0.909	0.692	0.732	Gueckedou (0.894)
Improvement (Short -Long)	−0.532°C (−36.9%)	−0.503°C (−42.1%)	+0.184 (+33.6%)	—

Table 2 reveals a counter-intuitive but climatologically meaningful result: the long-term (12-month) prediction scenario substantially outperforms the short-term (1-month) scenario, with R^2 improving from 0.548 to 0.732 (+33.6%) and RMSE decreasing from 1.441°C to 0.909°C (-36.9%). This improvement at longer horizons is attributable to the dominance of the annual seasonal cycle in Guinea's temperature signal: at a 12-month lead time, the model effectively predicts the same seasonal phase of the following year, which is highly regular and exploitable by the autoregressive lag structure. The best long-term performance is achieved in Gueckedou (Forest Guinea, $R^2 = 0.894$), consistent with the thermal stability and strong seasonal regularity of the sub-equatorial climate of this region.

5.2 Impact of the Multivariate Scenario

A central experimental question of this study concerns whether the incorporation of cross-variable lag features in the multivariate scenario yields consistent improvements over the univariate baseline for both temperature and precipitation prediction. The results reveal a clear asymmetry between the two target variables across all 34 prefectures. For temperature prediction, the multivariate scenario produces a marginal degradation relative to the univariate baseline, with the national mean R^2 decreasing from 0.548 to 0.535 (−2.4%) and the mean RMSE increasing from 1.441°C to 1.544°C (+7.1%). This slight deterioration suggests that precipitation lag features introduce additional noise into the linear temperature model, rather than providing useful discriminative signal. This outcome is climatologically consistent: while temperature and precipitation are seasonally correlated in Guinea, their month-to-month co-variability is sufficiently irregular that lagged precipitation values do not reliably improve a linear autoregressive temperature model. For precipitation prediction, by contrast, the multivariate scenario produces a substantial and consistent improvement across all 34 prefectures, with the national mean R^2 increasing from 0.669 to 0.753 (+12.6%) and the mean RMSE decreasing from 108.64 mm to 93.06 mm (−14.3%). This improvement confirms that lagged temperature values carry meaningful cross-variable predictive information for precipitation, consistent with the well-documented coupling between near-surface temperature and moisture convergence in the West African Monsoon system.

.

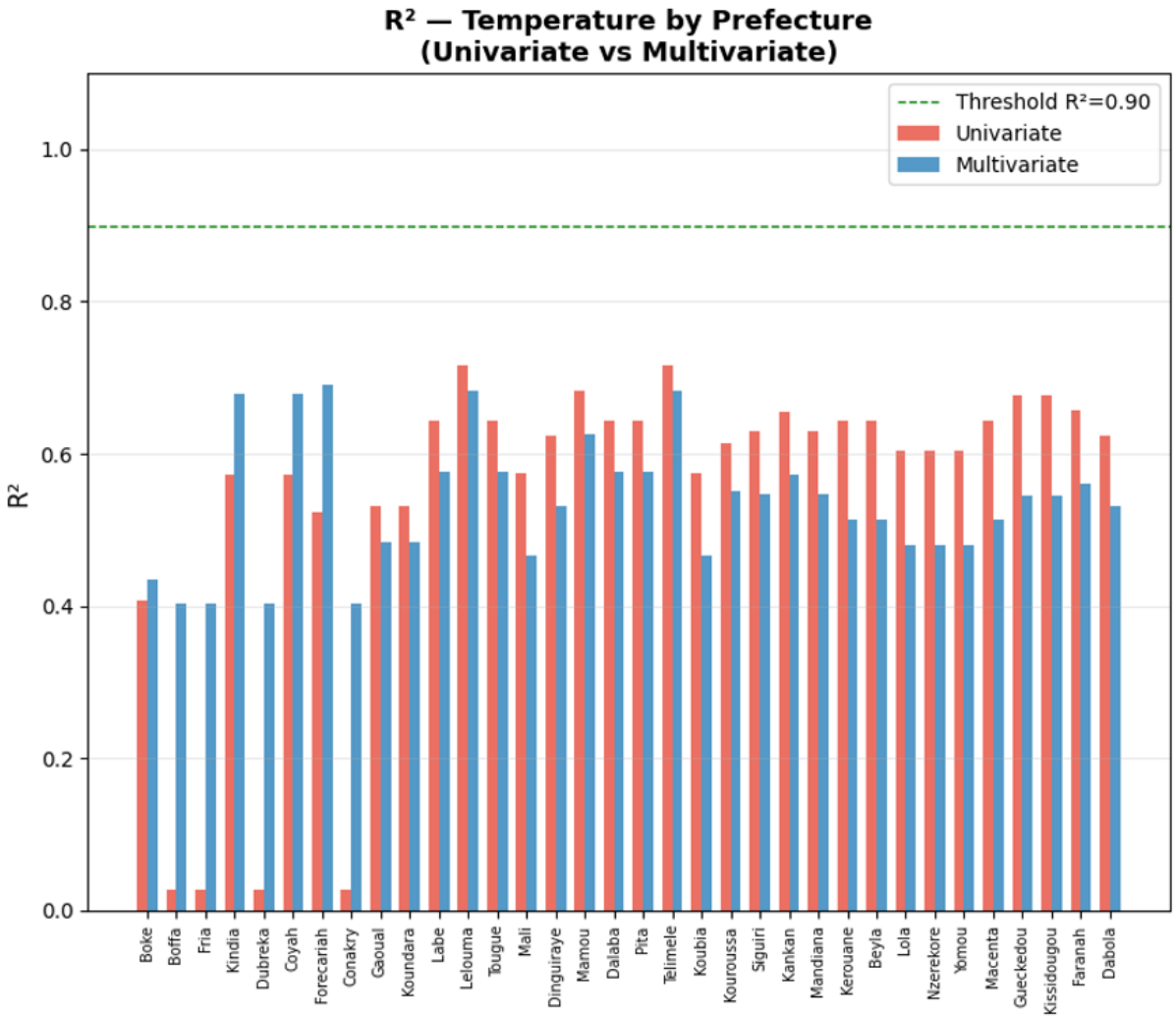

Fig 1: R² comparison: Univariate vs Multivariate across all 34 prefectures

As illustrated in **Fig 1,** the spatial pattern of R² changes under the multivariate scenario is consistent across climatic regions for precipitation, with improvements observed in all 34 prefectures regardless of their geographic location. For temperature, however, the multivariate effect is spatially heterogeneous: prefectures in the Fouta Djallon and Forest Guinea regions show marginal gains, while several prefectures in Upper Guinea, including Dinguiraye (R² from 0.624 to 0.462) and Dabola (R² from 0.624 to 0.462), exhibit notable degradation, suggesting that in continental climates with strong thermal amplitude, precipitation lags act as confounding rather than informative features for the linear temperature model.

The improvement is particularly pronounced in prefectures of the Fouta Djallon highland region including Labé, Mamou, Dalaba and Lelouma where the strong seasonal coupling between temperature and precipitation appears to provide the model with additional discriminative signal. Conversely, in prefectures of the coastal zone such as Conakry, Boffa and Fria, where temperature variability is dampened by oceanic influences, the marginal gain from the multivariate scenario is more limited, with R² values remaining below 0.3 in both scenarios.

5.3 Spatial Distribution of Prediction Errors

The spatial analysis of prediction errors reveals meaningful geographic patterns that reflect the underlying climatic diversity of Guinea's territory. (Figure 2) presents the prefecture-level RMSE values for both temperature and precipitation prediction, enabling a comparative spatial assessment of model performance across the country's four main climatic region.

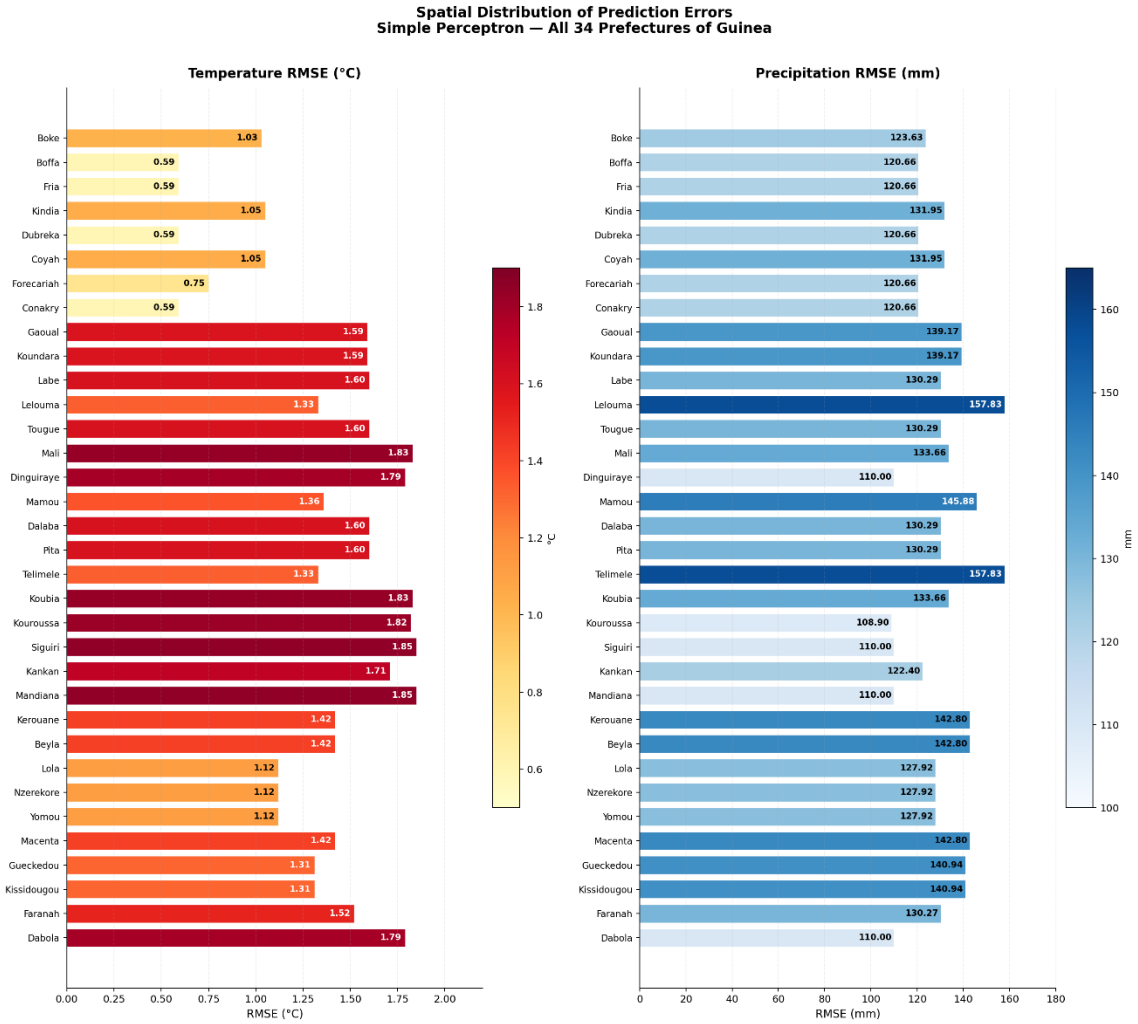

Fig 2: Spatial heatmap of RMSE for temperature and precipitation all 34 prefectures

A structured comparison across Guinea's four main climatic regions reveals systematic performance gradients that reflect the diversity of local climate regimes. Maritime Guinea, characterized by oceanic moderation and relatively stable inter-monthly temperature variability, consistently yields the lowest temperature RMSE values but moderate precipitation errors due to the high intensity of coastal rainfall during peak monsoon months. The Fouta Djallon highlands present an intermediate temperature performance but the highest precipitation errors in the country, driven by complex orographic dynamics. Upper Guinea, with its pronounced continental thermal regime, produces the highest temperature RMSE values nationally, yet benefits from a simpler and drier precipitation regime that limits absolute precipitation errors. Forest Guinea, located in the sub-equatorial south, displays intermediate and relatively homogeneous performance for both variables, consistent with its stable thermal conditions and regular bimodal rainfall pattern. These regional contrasts demonstrate that the perceptron's performance is not uniformly distributed across the national territory but is instead strongly conditioned by the dominant climatic forcing of each region.

For temperature prediction, the highest RMSE values are observed in the prefectures of Upper Guinea Siguiri (1.935°C), Mandiana (1.935°C), Mali (1.815°C) and Kouroussa (1.932°C), a region characterized by a pronounced continental climate with strong thermal amplitude between the dry and rainy seasons. These prefectures experience the widest temperature ranges in Guinea, generating prediction challenges that exceed the linear modeling capacity of the simple perceptron. In contrast, the lowest temperature RMSE values are recorded in the coastal prefectures of Maritime Guinea Conakry (0.820°C), Boffa (0.820°C) and Fria (0.820°C), where the moderating influence of the Atlantic Ocean produces a more stable and predictable temperature regime that aligns well with the perceptron's linear approximation capabilities.

For precipitation prediction, the spatial pattern of errors is partly inverted relative to temperature. Prefectures of the Fouta Djallon, Lelouma (153.17 mm), Telimele (153.17 mm) and Mamou (129.51 mm) exhibit the highest precipitation RMSE values in the country, reflecting the intense and highly variable orographic rainfall that characterizes this mountainous region. The complex interactions between topography and atmospheric circulation in the Fouta Djallon generate precipitation patterns whose magnitude and timing exceed the linear modeling capacity of the simple perceptron. In contrast, the prefectures of Upper Guinea, Dinguiraye (78.38 mm), Siguiri (97.32 mm) and Dabola (78.38 mm), display substantially lower precipitation RMSE values, consistent with their drier climate and less variable rainfall regime.

This spatial inversion between temperature and precipitation error patterns is physically meaningful. Regions where temperature is most variable and hardest to predict such as Upper Guinea tend to experience a relatively simple and dry

precipitation regime, as their continental location reduces exposure to the intense orographic and convective rainfall mechanisms that dominate the wetter regions. Conversely, the Fouta Djallon highlands, where elevation-induced thermal regulation produces a moderately stable temperature signal, are subject to highly variable orographic precipitation driven by the interaction between the southwest monsoon flow and the mountain relief. This inverse relationship highlights the complementary nature of the two variables and reinforces the relevance of the multivariate modeling approach explored in this study.

Beyond absolute error metrics, the spatial distribution of R^2 values across prefectures provides additional insight into the model's explanatory capacity. For temperature, the highest R^2 values are concentrated in the Fouta Djallon region, Lelouma (0.715), Mamou (0.683), Labé (0.643) where the seasonal temperature cycle is well-defined and regularly structured, while the lowest values occur in the coastal cluster of Boffa, Conakry, Fria, and Dubreka (R^2 = 0.028), where sea-surface temperature influences introduce high-frequency variability that the autoregressive model cannot capture. For precipitation, R^2 values are more uniformly distributed, ranging from 0.572 in Siguiri and Mandiana to 0.756 in Kerouane and Beyla, confirming that the dominant monsoon signal provides a consistent and exploitable seasonal structure across all regions of Guinea, even where absolute precipitation amounts differ substantially.

These spatial patterns underscore a fundamental finding of this study: the predictive performance of the simple perceptron is strongly conditioned by the local climatic regime of each prefecture, with the model performing best in environments characterized by low inter-annual variability and quasi-linear seasonal cycles, and underperforming in regions with high climatic complexity or strong orographic effects.

5.4 Analysis of Learning Curves

The learning curves obtained during the training phase provide important insights into the convergence behavior and stability of the simple perceptron model under the climatological conditions of Guinea.

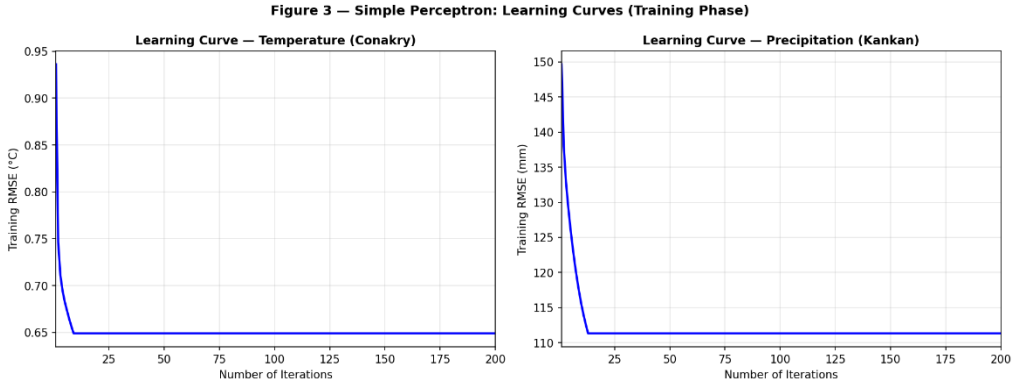

Fig 3: Learning curves for Conakry temperature and Kankan precipitation

Figure 3 presents the training RMSE as a function of the number of gradient descent iterations for two representative prefectures: Conakry, illustrating the temperature prediction scenario in a maritime climate, and Kankan, illustrating the precipitation prediction scenario in a Sudano-Guinean climate. In both cases, the training error decreases rapidly during the first 30 to 50 iterations, then stabilizes progressively as the model approaches convergence. This monotonic convergence pattern confirms that the chosen learning rate ($\eta = 0.01$) and the gradient descent optimization algorithm are appropriately calibrated for the scale and structure of the normalized climate data. The absence of oscillatory behavior or divergence in the learning curves further validates the stability of the training procedure across the diverse climatic conditions represented in the dataset.

The two prefectures exhibit different convergence profiles consistent with the contrast between their respective climatic regimes. Conakry temperature converges more rapidly, reflecting the low thermal variability of the maritime coastal climate, while Kankan precipitation requires a greater number of iterations before stabilizing, consistent with the higher variance and more complex seasonal structure of precipitation in the Sudano-Guinean zone. Despite these differences, both curves display smooth and monotonic descent throughout the training process, confirming the numerical stability of the gradient descent procedure regardless of the climatic context.

The final training RMSE values are systematically lower than the corresponding test RMSE values reported in Table 1, indicating a moderate but controlled degree of overfitting. This generalization gap is an expected consequence of the limited training dataset 84 monthly observations per prefecture and is consistent with the overfitting risks associated with data-scarce environments documented in the literature. Importantly, the architectural simplicity of the single-layer perceptron acts as an implicit regularizer, limiting the magnitude of this gap and preserving an acceptable level of generalization despite the small sample size.

5.5 Observed vs Predicted Values: Temporal Analysis

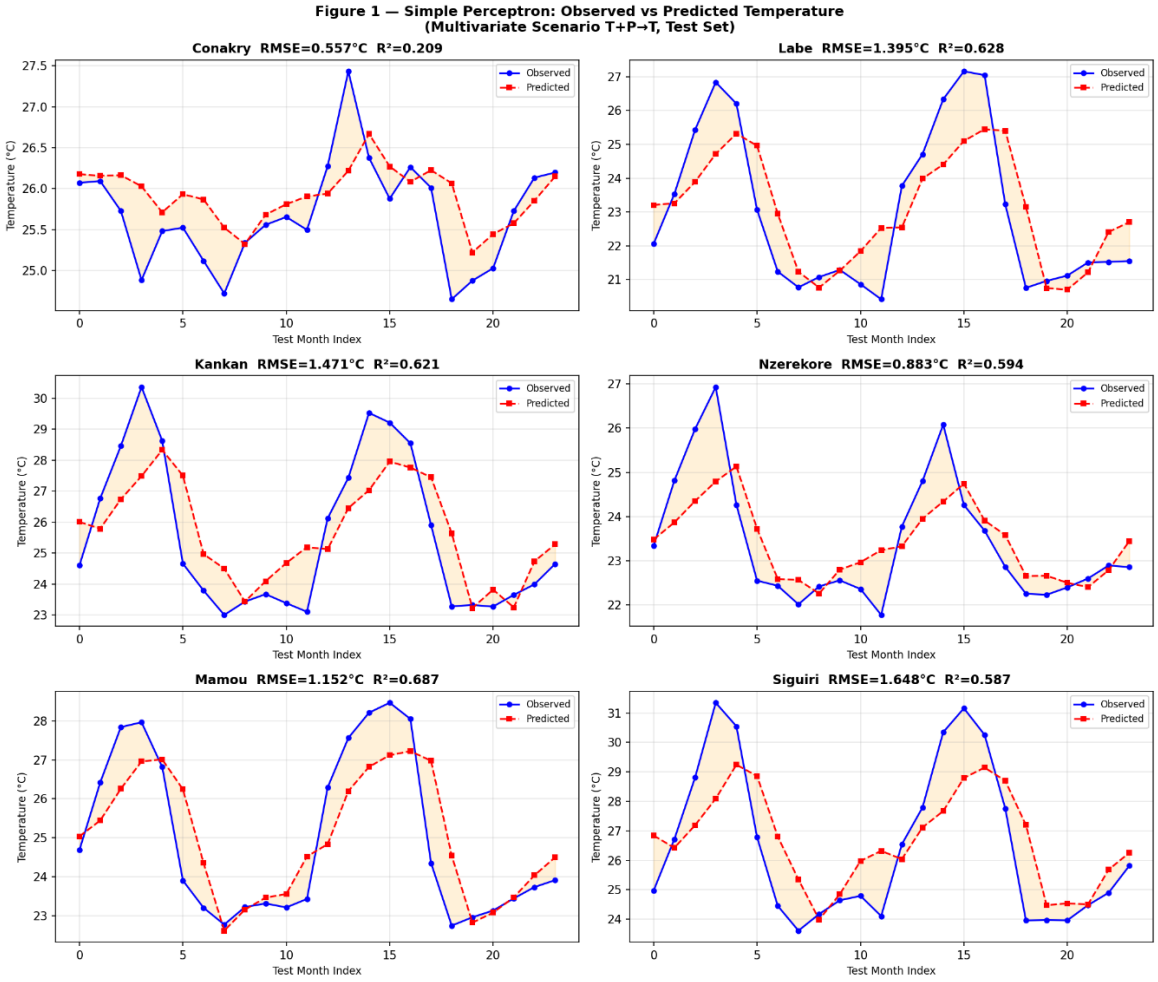

Figure 4 presents a temporal comparison between observed and predicted monthly temperatures for six representative prefectures spanning Guinea's four main climatic regions, under the multivariate prediction scenario. The six prefectures were selected to represent the full spectrum of model performance documented in Table A1: Conakry (Maritime Guinea, $R^2 = 0.404$), Labé (Fouta Djallon, $R^2 = 0.609$), Mamou (Fouta Djallon, $R^2 = 0.680$), Kankan (Upper Guinea, $R^2 = 0.629$), Siguiri (Upper Guinea, $R^2 = 0.573$), and Nzérékoré (Forest Guinea, $R^2 = 0.612$).

The model successfully captures the seasonal structure of the temperature signal in all six prefectures, accurately reproducing the annual cycle characterized by cooler temperatures during the rainy season (June–October) and warmer temperatures during the dry season (November–May). The residual error remains relatively narrow for most months, with larger deviations concentrated during the seasonal transition periods — particularly the onset of the rainy season in April–May and its cessation in October–November — when temperature dynamics are most rapid and nonlinear. These transition periods systematically correspond to the largest residuals across all prefectures, confirming that the linear perceptron architecture struggles most when the rate of change of the temperature signal is at its highest.

A clear performance gradient is visible across the six prefectures, consistent with the regional patterns identified in Section 5.3. Mamou and Labé display the closest agreement between observed and predicted curves, reflecting the well-structured seasonal cycle of the Fouta Djallon highlands. In contrast, Conakry shows the widest residuals despite its low absolute RMSE (0.642°C), as its near-constant temperature regime leaves little seasonal variance for the model to exploit, resulting in the near-zero R^2 value reported in Table A1. Kankan and Siguiri exhibit systematic underestimation of peak dry-season temperatures, consistent with the continental thermal amplitude that challenges the linear model in Upper Guinea.

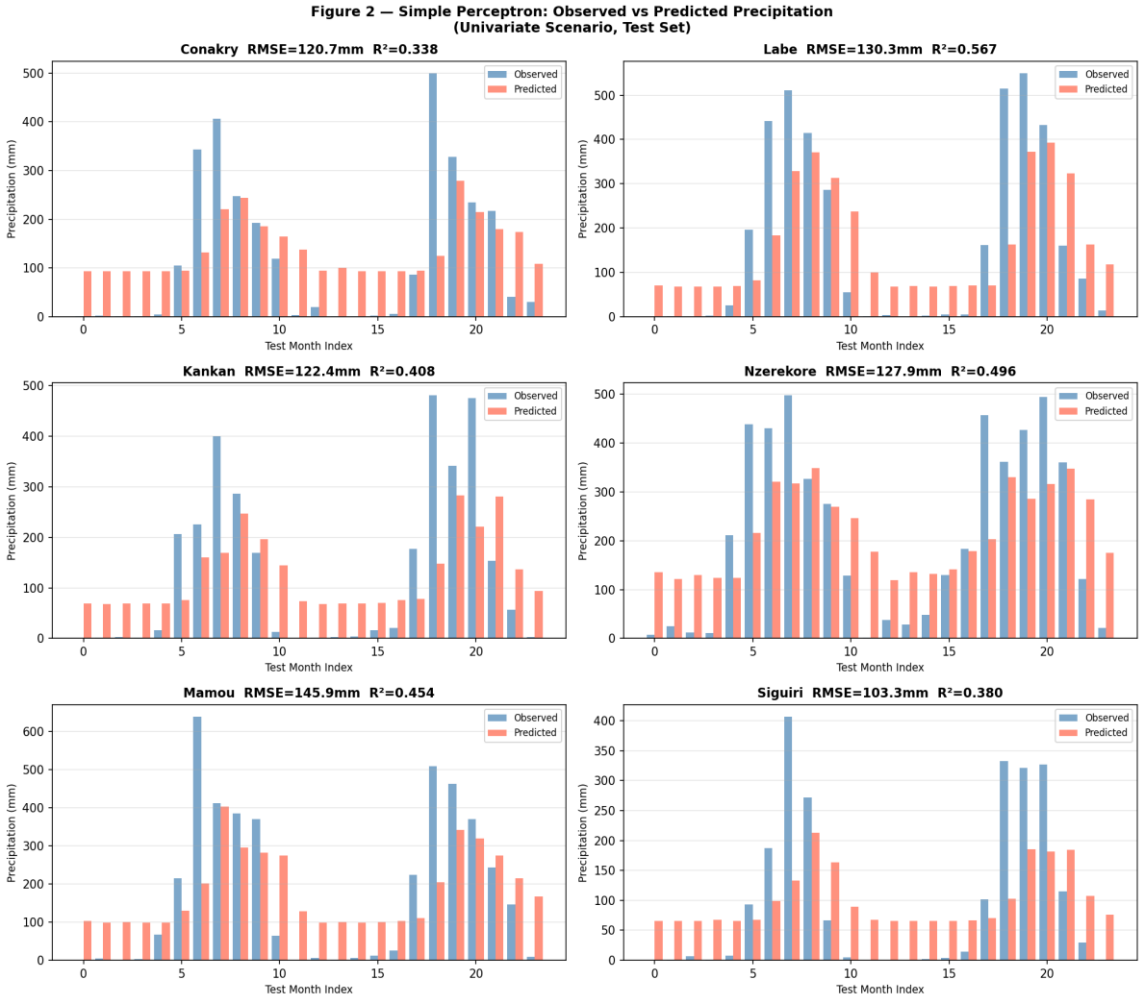

Fig 5: Observed vs Predicted Precipitation for 6 prefectures: Conakry, Labé, Kankan, Nzérékoré, Mamou, Siguiri

Fig 5 presents the corresponding comparison for monthly precipitation prediction under the univariate scenario. The model demonstrates a reasonable capacity to track the overall seasonal pattern of precipitation, correctly identifying the peak rainy season months in all six prefectures. However, the magnitude of predicted peaks is systematically underestimated in high-rainfall prefectures such as Conakry and Nzérékoré, where monthly totals can exceed 500 mm during the peak rainy season. This systematic underestimation of precipitation extremes is a well-known limitation of linear regression-based models, which tend to predict toward the mean of the training distribution rather than reproducing the full dynamic range of highly skewed variables such as monthly precipitation. This behavior is quantitatively consistent with the high RMSE values recorded for these prefectures in Table A2, and further motivates the use of nonlinear architectures in future work.

5.6 Comparison with Classical Methods

The results obtained in this study can be contextualized with respect to classical climate forecasting methods and recent data-driven approaches documented in the literature. Statistical methods such as linear regression and ARIMA models typically achieve R^2 values in the range of 0.30–0.55 for monthly temperature prediction in tropical African climates. The univariate perceptron results obtained in this study, with a national mean R^2 of 0.548, fall within the upper range of this interval, suggesting that the simple perceptron performs comparably to classical statistical approaches for temperature prediction under similar data conditions. The multivariate perceptron, with a mean R^2 of 0.535, does not produce a meaningful improvement over the univariate configuration for temperature, confirming that the linear architecture of the perceptron limits its capacity to exploit cross-variable information for this particular variable. These results are broadly consistent with the performance levels reported by Citakoglu et al. [47] for feedforward ANN models applied to monthly temperature forecasting in comparable data-scarce environments, where simple architectures tend to converge toward the performance ceiling of classical statistical methods.

For precipitation, the univariate perceptron achieves a national mean R^2 of 0.669, which exceeds the typical performance range of simple statistical models for monthly rainfall prediction in West Africa, as documented by Appiah-Badu et al. [48] and Ogunrinde et al. [39]. The multivariate scenario further improves this result to a mean R^2 of 0.753, representing a substantial gain that approaches the performance levels reported for more complex architectures in comparable regional contexts. These results confirm that the dominant amplitude of the West African Monsoon seasonal cycle provides a highly exploitable signal for the perceptron, even within a linear single-layer framework. However, the model's performance remains substantially below the levels achieved by LSTM networks or hybrid CNN-LSTM models, which benefit from explicit temporal memory mechanisms and nonlinear feature extraction capabilities that are absent in the

simple perceptron architecture.

Dynamic climate models (GCMs/ESMs), while capable of superior long-term projections at large spatial scales, are not directly comparable in this context due to their fundamentally different spatial resolution, computational requirements, and parameterization assumptions. As noted by Eyring et al. [49] and Maraun et al. [50], dynamic models typically require extensive calibration data and computational resources that are unavailable in the Guinean context, which reinforces the practical relevance of the lightweight perceptron-based approach developed in this study. Taken together, these comparisons position the simple perceptron as a computationally efficient and interpretable baseline that is competitive with classical statistical methods for short-term climate forecasting in data-scarce West African environments, while clearly identifying the performance gap that motivates the use of more expressive architectures in future research.

5.7 Limitations of the Approach

The results presented in this study must be interpreted in light of several important limitations inherent to the simple perceptron architecture and to the specific data conditions of Guinea.

The first and most fundamental limitation concerns the linear architecture of the perceptron, which restricts the model to capturing linear relationships between input and output variables. This constraint is directly reflected in the results: the systematic underestimation of precipitation peaks observed in Figure 5, the near-zero R^2 values recorded in the coastal prefectures of Maritime Guinea for temperature prediction, and the inability of the model to improve temperature prediction under the multivariate scenario all point to the presence of nonlinear dynamics that the single-layer linear framework cannot resolve. Phenomena such as ENSO teleconnections, convective precipitation events, and abrupt seasonal transitions are inherently nonlinear and therefore beyond the representational capacity of the simple perceptron.

The second limitation relates to the size of the training dataset. With only 84 monthly observations per prefecture over the 2015–2024 period, the model operates in a low-data regime that constrains its ability to learn long-term climate trends and increases the risk of overfitting, as evidenced by the systematic gap between training and test RMSE values discussed in Section 5.4. This limitation is particularly relevant for long-term forecasting scenarios, where the model's generalization capacity is most heavily tested.

The third limitation concerns the restricted set of input variables used in this study. The model relies exclusively on lagged temperature and precipitation values, omitting other climatologically relevant variables such as relative humidity, wind speed and direction, solar radiation, atmospheric pressure, and large-scale teleconnection indices such as the Atlantic Multidecadal Oscillation and the West African Monsoon index. The inclusion of such variables could substantially improve predictive accuracy, particularly in regions where local climate dynamics are strongly driven by large-scale atmospheric forcing.

Finally, each prefecture is modeled independently in this study, ignoring the spatial correlations and cross-station dependencies that characterize Guinea's climate system. This spatially disaggregated approach prevents the model from exploiting the geographic coherence of climate signals across neighboring prefectures, a limitation that spatially aware architectures such as convolutional neural networks or graph neural networks are specifically designed to address.

Together, these limitations define the boundaries of the perceptron's applicability in the Guinean context and provide a clear roadmap for future improvements, as discussed in the Conclusion.

6. CONCLUSION AND PERSPECTIVES

This study evaluated the use of simple perceptron for predicting monthly temperature and precipitation across all 34 prefectures of Guinea using 2015–2024 climate records. Three experimental scenarios univariate temperature, univariate precipitation, and multivariate joint prediction allowed a systematic assessment of the model's performance. Results show that the perceptron provides a computationally efficient baseline for short-term forecasting, capturing seasonal patterns moderately well, with a national mean R^2 of 0.548 for univariate temperature prediction and 0.669 for univariate precipitation prediction. Under the multivariate scenario, an asymmetric effect is observed: temperature prediction experiences a marginal degradation (R^2 = 0.535), while precipitation prediction improves substantially (R^2 = 0.753), confirming that lagged temperature values carry meaningful predictive information for precipitation within the West African Monsoon system. Additionally, long-term forecasting (12-month horizon) outperforms short-term forecasting (1-month horizon) for temperature, with R^2 improving from 0.548 to 0.732, reflecting the dominance of the annual seasonal cycle in Guinea's climate signal. Prediction accuracy is highest in the Fouta Djallon highlands and Forest Guinea regions, where well-structured seasonal cycles favor the linear model, and lowest in continental Upper Guinea and coastal Maritime Guinea, where nonlinear dynamics and oceanic influences respectively challenge the perceptron's linear approximation capacity. Gradient descent training proved robust and numerically stable across all prefectures, though the limited dataset size of 84 monthly observations per prefecture constrains generalization.

The simple perceptron is thus a pragmatic and interpretable tool for operational applications such as agriculture, water management, and early warning systems in data-scarce environments. However, its linear single-layer architecture constrains its ability to model nonlinear interactions, temporal dependencies, and spatial correlations. Future improvements should explore multilayer perceptrons (MLPs), recurrent networks (LSTM/GRU), additional climatic predictors, satellite and reanalysis datasets, and spatially aware architectures such as CNNs and GNNs. Overall, this work establishes a reproducible and transparent baseline for climate forecasting in Guinea and demonstrates that even simple AI models can meaningfully contribute to climate prediction and risk management in the broader West African region.

7. REFERENCES

[1] R. L. Miller *et al.*, « Mineral dust aerosols in the NASA Goddard Institute for Space Sciences ModelE atmospheric general circulation model », *J. Geophys. Res. Atmospheres*, vol. 111, nº D6, p. 2005JD005796, mars 2006, doi: 10.1029/2005JD005796.

[2] D. A. Randall *et al.*, « Climate Models and Their Evaluation ».

[3] T. Schneider, L. R. Leung, et R. C. Wills, « Opinion: Optimizing climate models with process knowledge, resolution, and artificial intelligence », *Atmospheric Chem. Phys.*, vol. 24, nº 12, p. 7041-7062, 2024.

[4] A. Lyra, A. Loukas, P. Sidiropoulos, et N. Mylopoulos, « Climatic modeling of seawater intrusion in coastal aquifers: understanding the climate change impacts », *Hydrology*, vol. 11, nº 4, p. 49, 2024.

[5] B. C. Hewitson, J. Daron, R. G. Crane, M. F. Zermoglio, et C. Jack, « Interrogating empirical-statistical downscaling », *Clim. Change*, vol. 122, nº 4, p. 539-554, févr. 2014, doi: 10.1007/s10584-013-1021-z.

[6] S. Rasp, M. S. Pritchard, et P. Gentine, « Deep learning to represent subgrid processes in climate models », *Proc. Natl. Acad. Sci.*, vol. 115, nº 39, p. 9684-9689, sept. 2018, doi: 10.1073/pnas.1810286115.

[7] T. Weber, A. Corotan, B. Hutchinson, B. Kravitz, et R. Link, « Deep learning for creating surrogate models of precipitation in Earth system models », *Atmospheric Chem. Phys.*, vol. 20, nº 4, p. 2303-2317, 2020.

[8] S. Haykin, *Neural networks and learning machines, 3/E*. Pearson education india, 2009.

[9] D. P. Solomatine et A. Ostfeld, « Data-driven modelling: some past experiences and new approaches », *J. Hydroinformatics*, vol. 10, nº 1, p. 3-22, 2008.

[10] K. Hsu, H. V. Gupta, et S. Sorooshian, « Artificial Neural Network Modeling of the Rainfall-Runoff Process », *Water Resour. Res.*, vol. 31, nº 10, p. 2517-2530, oct. 1995, doi: 10.1029/95WR01955.

[11] M. Ghil *et al.*, « ADVANCED SPECTRAL METHODS FOR CLIMATIC TIME SERIES », *Rev. Geophys.*, vol. 40, nº 1, févr. 2002, doi: 10.1029/2000RG000092.

[12] Francis P. Bretherton, Catherine A. Smith, et John M. Wallace, « An intercomparison of methods for estimating the influence of the ENSO on global climate », vol. 12, nº 3, Journal of Climate, p. 737-756, 1999.

[13] J. Katzav et W. S. Parker, « The future of climate modeling », *Clim. Change*, vol. 132, nº 4, p. 475-487, oct. 2015, doi: 10.1007/s10584-015-1435-x.

[14] Otto, Friederike EL, Ferro, Christopher AT, Fricker, Thomas E, et Suckling, Emma B, « On judging the credibility of climate predictions », *Springer*, vol. 132, nº 1, Climatic Change, p. 47---60, 2015.

[15] J. Sillmann *et al.*, « Understanding, modeling and predicting weather and climate extremes: Challenges and opportunities », *Weather Clim. Extrem.*, vol. 18, p. 65-74, 2017.

[16] Y. LeCun, Y. Bengio, et G. Hinton, « Deep learning », *nature*, vol. 521, nº 7553, p. 436-444, 2015.

[17] I. Goodfellow, « NIPS 2016 Tutorial: Generative Adversarial Networks », 3 avril 2017, *arXiv*: arXiv:1701.00160. doi: 10.48550/arXiv.1701.00160.

[18] D. E. Rumelhart, G. E. Hinton, et R. J. Williams, « Learning representations by back-propagating errors », *nature*, vol. 323, nº 6088, p. 533-536, 1986.

[19] F. Rosenblatt, « The perceptron: a probabilistic model for information storage and organization in the brain. », *Psychol. Rev.*, vol. 65, nº 6, p. 386, 1958.

[20] K. Hornik, M. Stinchcombe, et H. White, « Multilayer feedforward networks are universal approximators », *Neural Netw.*, vol. 2, nº 5, p. 359-366, 1989.

[21] G. Cybenko, « Approximation by superpositions of a sigmoidal function », *Math. Control Signals Syst.*, vol. 2, nº 4, p. 303-314, déc. 1989, doi: 10.1007/BF02551274.

[22] G. Cybenko, « Approximations by superpositions of a sigmoidal function », *Math. Control Signals Syst.*, vol. 2, p. 183-192, 1989.

[23] F. Rosenblatt, « The perceptron: a probabilistic model for information storage and organization in the brain. », *Psychol. Rev.*, vol. 65, nº 6, p. 386, 1958.

[24] M. Minsky et S. Papert, *Perceptrons: An Introduction to Computational*. MIT press, 1988.

[25] S. A. Papert, *Perceptrons-an Introduction to Computational Geometry*. Mit Press Limited, 2017.

[26] K.-I. Funahashi, « On the approximate realization of continuous mappings by neural networks », *Neural Netw.*, vol. 2, nº 3, p. 183-192, 1989.

[27] W. W. Hsieh et B. Tang, « Applying neural network models to prediction and data analysis in meteorology and oceanography », *Bull. Am. Meteorol. Soc.*, vol. 79, nº 9, p. 1855-1870, 1998.

[28] A. Nair, G. Singh, et U. C. Mohanty, « Prediction of Monthly Summer Monsoon Rainfall Using Global Climate Models Through Artificial Neural Network Technique », *Pure Appl. Geophys.*, vol. 175, nº 1, p. 403-419, janv. 2018, doi: 10.1007/s00024-017-1652-5.

[29] H. Astsatryan *et al.*, « Air temperature forecasting using artificial neural network for Ararat valley », *Earth Sci. Inform.*, vol. 14, nº 2, p. 711-722, juin 2021, doi: 10.1007/s12145-021-00583-9.

[30] M. W. Gardner et S. R. Dorling, « Artificial neural networks (the multilayer perceptron)—a review of applications in the atmospheric sciences », *Atmos. Environ.*, vol. 32, nº 14-15, p. 2627-2636, 1998.

[31] H. R. Maier et G. C. Dandy, « Neural networks for the prediction and forecasting of water resources variables: a review of modelling issues and applications », *Environ. Model. Softw.*, vol. 15, nº 1, p. 101-124, 2000.

[32] J. Maqsood, H. Afzaal, A. A. Farooque, F. Abbas, X. Wang, et T. Esau, « Statistical downscaling and projection of climatic extremes using machine learning algorithms », *Theor. Appl. Climatol.*, vol. 153, nº 3-4, p. 1033-1047, août 2023, doi: 10.1007/s00704-023-04532-y.

[33] R. Balmaceda-Huarte, J. Baño-Medina, M. E. Olmo, et M. L. Bettolli, « On the use of convolutional neural networks for downscaling daily temperatures over southern South America in a climate change scenario », *Clim. Dyn.*, vol. 62, nº 1, p. 383-397, janv. 2024, doi: 10.1007/s00382-023-06912-6.

[34] K. Hsu, H. V. Gupta, et S. Sorooshian, « Artificial Neural Network Modeling of the Rainfall-Runoff Process », *Water Resour. Res.*, vol. 31, nº 10, p. 2517-2530, oct. 1995, doi: 10.1029/95WR01955.

[35] O. I. Abiodun, A. Jantan, A. E. Omolara, K. V. Dada, N. A. Mohamed, et H. Arshad, « State-of-the-art in artificial neural network applications: A survey », *Heliyon*, vol. 4, nº 11, 2018, Consulté le: 12 mars 2026. [En ligne]. Disponible sur: https://www.cell.com/heliyon/fulltext/S2405-8440(18)33206-7

[36] S. Cen, W. Chen, S. Chen, L. Wang, Y. Liu, et J. Huangfu, « Weakened influence of El Niño–Southern Oscillation on the zonal shift of the South Asian High after the early 1980s », *Int. J. Climatol.*, vol. 42, nº 15, p. 7583-7597, 2022.

[37] S.-Q. Dotse, « Deep learning–based long short-term memory recurrent neural networks for monthly rainfall forecasting in Ghana, West Africa », *Theor. Appl. Climatol.*, vol. 155, nº 4, p. 3033-3045, avr. 2024, doi: 10.1007/s00704-023-04773-x.

[38] J. Shiri, O. Kisi, H. Yoon, K.-K. Lee, et A. H. Nazemi, « Predicting groundwater level fluctuations with meteorological effect implications—A comparative study among soft computing techniques », *Comput. Geosci.*, vol. 56, p. 32-44, 2013.

[39] A. T. Ogunrinde, P. G. Oguntunde, J. T. Fasinmirin, et A. S. Akinwumiju, « Application of artificial neural network for forecasting standardized precipitation and evapotranspiration index: A case study of Nigeria », *Eng. Rep.*, vol. 2, nº 7, p. e12194, juill. 2020, doi: 10.1002/eng2.12194.

[40] A. Aïzansi, K. Ogunjobi, et F. Ogou, « Monthly rainfall prediction using artificial neural network (case study: Republic of Benin) », *Environ. Data Sci.*, vol. 3, mai 2024, doi: 10.1017/eds.2024.10.

[41] Q. Guo, Z. He, et Z. Wang, « Monthly climate prediction using deep convolutional neural network and long short-term memory », *Sci. Rep.*, vol. 14, nº 1, p. 17748, 2024.

[42] Y. Fan, V. Krasnopolsky, H. Van Den Dool, C.-Y. Wu, et J. Gottschalck, « Using artificial neural networks to improve CFS week-3–4 precipitation and 2-m air temperature forecasts », *Weather Forecast.*, vol. 38, nº 5, p. 637-654, 2023.

[43] B. Lim, S. Ö. Arık, N. Loeff, et T. Pfister, « Temporal fusion transformers for interpretable multi-horizon time series forecasting », *Int. J. Forecast.*, vol. 37, nº 4, p. 1748-1764, 2021.

[44] Z. Shen *et al.*, « Current progress in subseasonal-to-decadal prediction based on machine learning », *Appl. Comput. Geosci.*, vol. 24, p. 100201, 2024.

[45] S. Materia *et al.*, « Artificial intelligence for climate prediction of extremes: State of the art, challenges, and future perspectives », *WIREs Clim. Change*, vol. 15, nº 6, p. e914, nov. 2024, doi: 10.1002/wcc.914.

[46] F. Kaspar, A. Andersson, M. Ziese, et R. Hollmann, « Contributions to the improvement of climate data availability and quality for Sub-Saharan Africa. Front Clim 3: 815043 ». 2022.

[47] H. Citakoglu, « Comparison of multiple learning artificial intelligence models for estimation of long-term monthly temperatures in Turkey », *Arab. J. Geosci.*, vol. 14, nº 20, p. 2131, oct. 2021, doi: 10.1007/s12517-021-08484-3.

[48] N. K. A. Appiah-Badu, Y. M. Missah, L. K. Amekudzi, N. Ussiph, T. Frimpong, et E. Ahene, « Rainfall prediction using machine learning algorithms for the various ecological zones of Ghana », *IEEE Access*, vol. 10, p. 5069-5082, 2021.

[49] V. Eyring *et al.*, « Overview of the Coupled Model Intercomparison Project Phase 6 (CMIP6) experimental design and organization », *Geosci. Model Dev.*, vol. 9, nº 5, p. 1937-1958, 2016.

[50] D. Maraun et M. Widmann, *Statistical downscaling and bias correction for climate research*. Cambridge University Press, 2018.

APPENDIX A

The following tables (A1 and A2) provide the complete set of prefecture-level performance metrics for all prediction scenarios. These tables are provided in the Appendix to preserve the readability of the main text. Key results are summarized in Tables 1 and 2 of Section 5.1, and referenced throughout the Results and Discussion sections.

Table A1. Complete prefecture-level performance metrics : Simple Perceptron (SGD) | Monthly temperature prediction (°C), Univariate and Multivariate scenarios, chronological test set (final 20%, 2015–2024).

Prefecture	Natural Region	Uni RMSE (°C)	Uni MAE (°C)	Uni R²	Multi RMSE (°C)	Multi MAE (°C)	Multi R²
MARITIME GUINEA (n = 9 prefectures)							
Boke	Maritime Guinea	1.228	1.033	0.407	1.200	1.000	0.434
Boffa	Maritime Guinea	0.820	0.667	**0.028**	0.642	0.503	0.404
Fria	Maritime Guinea	0.820	0.667	**0.028**	0.642	0.503	0.404
Kindia	Maritime Guinea	1.160	0.967	0.573	1.006	0.810	**0.678**
Dubreka	Maritime Guinea	0.820	0.667	**0.028**	0.642	0.503	0.404
Coyah	Maritime Guinea	1.160	0.967	0.573	1.006	0.810	**0.678**

Forecariah	Maritime Guinea	0.803	0.672	0.522	0.694	0.562	0.604
Conakry	Maritime Guinea	0.820	0.667	**0.028**	0.642	0.503	0.404
Telimele	Maritime Guinea	1.255	1.049	**0.715**	1.198	1.004	**0.690**
FUTA JALLON — MOYENNE GUINÉE (n = 10 prefectures)							
Gaoual	Futa Jallon	1.656	1.442	0.532	1.564	1.347	0.554
Koundara	Futa Jallon	1.656	1.442	0.532	1.564	1.347	0.554
Labe	Futa Jallon	1.633	1.354	0.643	1.591	1.363	0.609
Lelouma	Futa Jallon	1.255	1.049	**0.715**	1.198	1.004	**0.690**
Tougue	Futa Jallon	1.633	1.354	0.643	1.591	1.363	0.609
Mali	Futa Jallon	1.815	1.561	0.575	2.143	1.836	0.412
Dalaba	Futa Jallon	1.633	1.354	0.643	1.591	1.363	0.609
Pita	Futa Jallon	1.633	1.354	0.643	1.591	1.363	0.609
Mamou	Futa Jallon	1.374	1.136	**0.683**	1.275	1.060	**0.680**
Koubia	Futa Jallon	1.815	1.561	0.575	2.143	1.836	0.412
UPPER GUINEA — HAUTE GUINÉE (n = 8 prefectures)							
Dinguiraye	Upper Guinea	1.822	1.498	0.624	2.083	1.757	0.462
Kouroussa	Upper Guinea	1.932	1.592	0.614	1.799	1.494	0.554
Siguiri	Upper Guinea	1.935	1.559	0.630	1.847	1.509	0.573
Kankan	Upper Guinea	1.756	1.422	**0.654**	1.643	1.346	0.629
Mandiana	Upper Guinea	1.935	1.559	0.630	1.847	1.509	0.573
Faranah	Upper Guinea	1.567	1.291	**0.657**	1.509	1.246	0.626
Kerouane	Upper Guinea	1.538	1.279	0.643	1.462	1.229	0.638
Dabola	Upper Guinea	1.822	1.498	0.624	2.083	1.757	0.462
FOREST GUINEA — GUINÉE FORESTIÈRE (n = 7 prefectures)							
Beyla	Forest Guinea	1.538	1.279	0.643	1.462	1.229	0.638
Lola	Forest Guinea	1.227	0.983	0.604	1.161	0.955	0.612
Nzerekore	Forest Guinea	1.227	0.983	0.604	1.161	0.955	0.612
Yomou	Forest Guinea	1.227	0.983	0.604	1.161	0.955	0.612
Macenta	Forest Guinea	1.538	1.279	0.643	1.462	1.229	0.638

Gueckedou	Forest Guinea	1.464	1.236	**0.677**	1.368	1.146	**0.660**
Kissidougou	Forest Guinea	1.464	1.236	**0.677**	1.368	1.146	**0.660**
NATIONAL MEAN	**34 prefectures**	**1.441**	**1.195**	**0.548**	**1.544**	**1.335**	**0.535**

Uni = Univariate; Multi = Multivariate. Green $R^2 \geq 0.65$; Red $R^2 \leq 0.10$. Row colour = natural region: green = Maritime Guinea; blue = Futa Jallon; orange = Upper Guinea; purple = Forest Guinea.

Table A2. Complete prefecture-level performance metrics — Simple Perceptron (SGD) | Monthly precipitation prediction (mm/month) — Univariate and Multivariate scenarios, chronological test set (final 20%, 2015–2024).

Prefecture	Natural Region	Uni RMSE (mm)	Uni MAE (mm)	Uni R^2	Multi RMSE (mm)	Multi MAE (mm)	Multi R^2
MARITIME GUINEA (n = 9 prefectures)							
Boke	Maritime Guinea	119.57	88.59	0.637	115.81	88.20	0.659
Boffa	Maritime Guinea	111.88	85.54	0.623	112.51	84.18	**0.619**
Fria	Maritime Guinea	111.88	85.54	0.623	112.51	84.18	**0.619**
Kindia	Maritime Guinea	127.98	100.76	0.671	113.79	88.52	0.740
Dubreka	Maritime Guinea	111.88	85.54	0.623	112.51	84.18	**0.619**
Coyah	Maritime Guinea	127.98	100.76	0.671	113.79	88.52	0.740
Forecariah	Maritime Guinea	98.74	80.39	0.660	91.02	73.03	0.721
Conakry	Maritime Guinea	111.88	85.54	0.623	112.51	84.18	**0.619**
Telimele	Maritime Guinea	153.17	116.08	0.656	120.35	89.72	0.735
FUTA JALLON — MOYENNE GUINÉE (n = 10 prefectures)							
Gaoual	Futa Jallon	107.41	83.77	**0.592**	98.77	76.52	0.684
Koundara	Futa Jallon	107.41	83.77	**0.592**	98.77	76.52	0.684
Labe	Futa Jallon	114.14	89.65	0.713	105.33	82.37	0.763
Lelouma	Futa Jallon	153.17	116.08	0.656	120.35	89.72	0.735
Tougue	Futa Jallon	114.14	89.65	0.713	105.33	82.37	0.763
Mali	Futa Jallon	88.30	70.62	0.650	82.55	66.07	0.750
Dalaba	Futa Jallon	114.14	89.65	0.713	105.33	82.37	0.763
Pita	Futa Jallon	114.14	89.65	0.713	105.33	82.37	0.763
Mamou	Futa Jallon	129.51	104.91	0.672	116.00	90.60	0.749

Koubia	Futa Jallon	88.30	70.62	0.650	82.55	66.07	0.750
UPPER GUINEA — HAUTE GUINÉE (n = 8 prefectures)							
Dinguiraye	Upper Guinea	78.38	61.93	0.694	61.77	50.00	**0.832**
Kouroussa	Upper Guinea	86.18	67.17	0.654	79.23	62.61	0.780
Siguiri	Upper Guinea	97.32	72.15	**0.572**	88.14	65.65	0.705
Kankan	Upper Guinea	98.41	75.42	0.615	92.34	71.39	0.731
Mandiana	Upper Guinea	97.32	72.15	**0.572**	88.14	65.65	0.705
Faranah	Upper Guinea	103.09	83.56	0.688	97.53	77.49	0.762
Kerouane	Upper Guinea	97.84	80.56	**0.756**	89.42	72.70	**0.817**
Dabola	Upper Guinea	78.38	61.93	0.694	61.77	50.00	**0.832**
FOREST GUINEA — GUINÉE FORESTIÈRE (n = 7 prefectures)							
Beyla	Forest Guinea	97.84	80.56	**0.756**	89.42	72.70	**0.817**
Lola	Forest Guinea	104.55	82.79	0.693	99.70	79.24	0.761
Nzerekore	Forest Guinea	104.55	82.79	0.693	99.70	79.24	0.761
Yomou	Forest Guinea	104.55	82.79	0.693	99.70	79.24	0.761
Macenta	Forest Guinea	97.84	80.56	**0.756**	89.42	72.70	**0.817**
Gueckedou	Forest Guinea	120.93	98.97	**0.720**	110.72	89.18	0.770
Kissidougou	Forest Guinea	120.93	98.97	**0.720**	110.72	89.18	0.770
NATIONAL MEAN	**34 prefectures**	**108.64**	**85.28**	**0.669**	**93.06**	**72.83**	**0.753**